

Temperature dependence of terahertz emission from InMnAs

Hui Zhan, Jason Deibel, Jonathan Laib, Chanjuan Sun,
Junichiro Kono, and Daniel M. Mittleman^{a)}

Department of Electrical and Computer Engineering, MS-366, Rice University, 6100 Main St., Houston, Texas 77005

Hiro Munekata

Imaging Science and Engineering Laboratory, Tokyo Institute of Technology, Yokohama 226-8502, Japan

(Received 6 September 2006; accepted 29 November 2006; published online 2 January 2007)

We have studied the terahertz radiation emitted by the dilute magnetic semiconductor InMnAs under femtosecond laser illumination, as a function of temperature. We observe a reversal of the polarity of the emitted terahertz field as the temperature is decreased, in both *p*-type and *n*-type materials. This effect is not observed in *p*-InAs. A competition between two oppositely directed currents, the photo-Dember current and the surface-field-induced current, can explain the observed polarity reversal. In contrast to nonmagnetic materials, these two currents are of comparable magnitude because the Mn impurity substantially reduces the carrier mobility in dilute magnetic semiconductors. © 2007 American Institute of Physics. [DOI: 10.1063/1.2425024]

Dilute magnetic semiconductors (DMSs) based on III-V compounds, which were produced in 1989,^{1,2} have inspired much interest in recent years. III-V DMSs are attractive candidates for studying dynamical processes in magnetically ordered systems, due to the clear distinction between mobile carriers and localized spins in the III-V semiconductors.^{3,4} They also show great potential for use in spintronic applications.^{1,2} Such applications will require a detailed understanding of the carrier dynamics, spin magnetism, and, in particular, their interactions in these materials. Terahertz emission spectroscopy is a powerful technique for studying ultrafast charge carrier dynamics in semiconductors. Many studies have examined terahertz emission from a variety of III-V semiconductors surface, including InAs, InSb, InP, and GaAs.⁵⁻¹¹ In particular, magnetic-field-induced enhancement of terahertz radiation from nonmagnetic semiconductor surfaces has been investigated thoroughly.¹¹⁻¹⁶ Recently, terahertz emission from ferromagnetic metal films^{17,18} and from the dilute ferromagnetic semiconductor GaMnAs (Ref. 19) have also been demonstrated. However, so far there have been no studies of InMnAs, one of the earliest III-V DMSs ever grown.

In this letter, we report terahertz emission from InAs-based DMS samples. This work builds on the large body of literature related to terahertz emission from InAs.^{5-7,11,13,20,21} We have observed a temperature-induced polarity reversal of the terahertz radiation from both *p*-InMnAs and *n*-InMnAs, in contrast to what has been previously observed in *p*-InAs.^{6,7} We attribute the observed polarity reversal of the terahertz radiation to the competition between two oppositely directed sources of photoinduced current: the surface-field-induced current and the photo-Dember effect. Due to the presence of the Mn dopant, the photo-Dember effect in InMnAs is much weaker than in InAs. As a result, the dominant terahertz radiation mechanism in InMnAs switches from the surface field current at high temperature to the photo-Dember effect at low temperature, leading to a change in the polarity of the emitted terahertz field. This result is reminis-

cent of the competition between displacement and transport currents in bulk GaAs, which manifests itself as a polarity reversal as a function of pump laser wavelength.²²

The samples used in our study are a 960-nm-thick *p*-In_{1-x}Mn_xAs sample and a 2- μ m-thick *n*-In_{1-x}Mn_xAs sample with the same Mn concentration, $x=0.025$. Both samples were grown by low-temperature molecular beam epitaxy on semi-insulating GaAs substrates at 300 and 200 °C, respectively. The Curie temperature of the *p*-InMnAs sample is 4 K, while the *n*-InMnAs sample exhibits no ferromagnetism down to 1.5 K.⁴ For comparison, we also study a *p*-InAs sample with doping concentration of 1×10^{16} cm⁻³. Our terahertz emission spectrometer uses a reflection configuration. A Ti: sapphire laser provides ultrafast laser pulses with $\lambda=800$ nm at a 76 MHz repetition rate and with a pulse duration of less than 80 fs. The pump beam is incident on the sample surface at an angle of 45° with a beam diameter of about 1 mm. Terahertz radiation is emitted from the samples in the specular reflection direction and detected using electro-optic sampling in a 1-mm-thick ZnTe crystal. The samples are held in a cryostat with windows transparent to both optical and terahertz radiations. The magnetically doped layers are thick compared to the optical penetration depth, so substrate effects can be ignored.

Figure 1 shows the time-domain terahertz waveforms emitted from the *p*-InMnAs sample, illustrating the

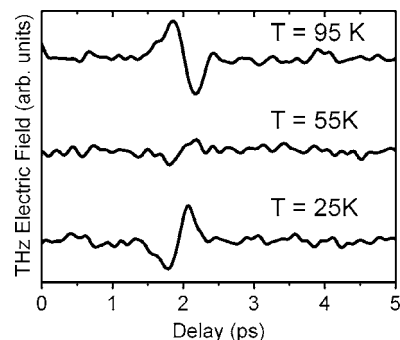


FIG. 1. Time-domain waveforms of terahertz radiation emitted from *p*-InMnAs at different temperatures.

^{a)}Electronic mail: daniel@rice.edu

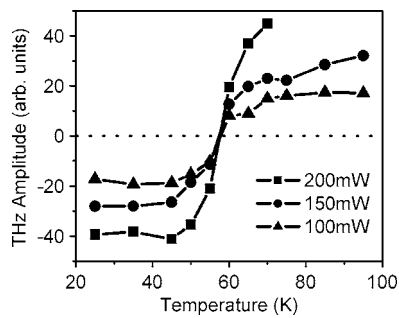


FIG. 2. Temperature dependence of the peak-to-peak amplitude of the emitted terahertz pulse from *p*-InMnAs at different pump powers. These correspond to excitation fluences of 132, 197, and 263 nJ/cm². A polarity reversal is observed at a temperature of ~ 57 K, independent of fluence.

temperature-dependent polarity reversal. We note that the shapes of the terahertz waveforms at the higher and lower temperatures are quite similar, as are the spectra (not shown). Figure 2 shows the amplitude of the emitted terahertz pulse as a function of temperature for several different excitation fluences. When cooling down the sample from room temperature, the amplitude of terahertz radiation signal decreases only slightly until ~ 100 K. Starting from this point, the amplitude decreases more rapidly, and eventually the polarity reverses at a temperature of ~ 57 K. We observe no significant effect of the polarization of the incident optical beam, which indicates that optical rectification does not contribute to the signal at these excitation densities.

Figure 3 shows the analogous time-domain waveforms from the *n*-type sample at different temperatures; the inset shows the temperature dependence at a fixed pump power. Here, we again observe a polarity reversal of the terahertz waveforms as a function of temperature. The polarity of the terahertz radiation from *n*-InMnAs is the same as that from *p*-InMnAs at both high temperature and low temperature. However, the temperature at which the polarity reverses is somewhat higher in *n*-InMnAs, around 70 K.

The fact that *n*-InMnAs and *p*-InMnAs show similar polarity reversals is somewhat surprising, because it suggests that the surface field current and photo-Dember current are directed opposite to each other in both of these materials. In most semiconductors, the surface depletion field is directed *into* the surface for *p* doping and *out of* the surface for *n* doping, while the photo-Dember effect always generates a transient current directed out of the semiconductor surface. One would expect these two effects to counteract each other in *p*-type semiconductors but to add in the case of *n*-type materials. However, previous work^{20,21} suggests that InAs is an exception to this rule. For InAs, the surface energy bands bend downward regardless of the sign of the dopant, due to the formation of an accumulation layer at the surface. As a result of the formation of this accumulation layer, changing the sign of the dopant does not change the direction of the surface depletion field.^{6,7,11} Thus, the surface field current and the photo-Dember current can indeed counteract each other in both *n*-InMnAs and *p*-InMnAs.

The magnetic impurity seems to have a significant influence on the ultrafast carrier dynamics in these DMS materials. No temperature-dependent polarity reversal is observed in *p*-InAs, since the emission mechanism is dominated by the photo-Dember effect at all temperatures.^{5-7,11} The distinct behavior of the DMS materials originates from the influence

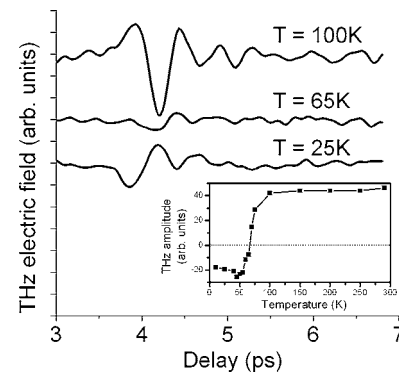


FIG. 3. Time-domain waveforms of terahertz radiation emitted from *n*-InMnAs at different temperatures. Inset: Temperature dependence of the peak-to-peak amplitude of the emitted terahertz pulse from *n*-InMnAs, with pump power of 200 mW. A polarity reversal is observed at a temperature of ~ 70 K.

of the Mn dopant on the carrier mobility, doping density, and the impurity level of the deep impurity. As the temperature decreases, the increase in the carrier mobility in InMnAs contributes to the increase of both the surface field current and the photo-Dember current. However, the decrease of the carrier density enhances the photo-Dember effect but reduces the surface depletion field. Also, the surface depletion width increases with decreasing temperature. So the enhancement of the surface field current by the increasing carrier mobility is counteracted by the temperature dependence of the surface depletion field and the depletion width. As a result, the surface field current has a much weaker temperature dependence than the photo-Dember current.^{5,8} As temperature decreases, the photo-Dember effect eventually becomes large enough to offset the surface field current, and so the emitted terahertz signal vanishes. As the temperature decreases further, the photo-Dember effect becomes the dominant mechanism. We note that the polarity of the terahertz emission from both *n*-InMnAs and *p*-InMnAs at low temperature is the same as the polarity of the terahertz emission from *p*-InAs. This is consistent with the above description in which the emission mechanism is the same (i.e., the photo-Dember effect) in these cases.

We use a simple model to analyze the transient photoinduced current. The drift current J_E and the diffusion current J_D are described by⁹

$$J_E = eE_s(N_n\mu_n + N_p\mu_p), \quad (1)$$

$$J_D = e(D_n \nabla N_n - D_p \nabla N_p). \quad (2)$$

The net effective transient current is the sum of these two contributions which, as noted above, are oppositely directed in our samples. Here, $N_n(N_p)$ is the total density of electrons (holes) including both hot and cold carriers⁷ and $\mu_n(\mu_p)$ is their mobility. The diffusion coefficient is defined by the Einstein relation as $D_i = \mu_i k_B T_i / e$, where T_i is the corresponding carrier temperature, approximated from the excess carrier energy $h\nu - E_G$. E_s is the maximum electric field at the sample surface, given by the Schottky model:⁸

$$E_s = \left(\frac{2eN_s\phi_s}{\epsilon_0\epsilon} \right)^{1/2}. \quad (3)$$

Here N_s is the static carrier density and ϕ_s is the band-bending potential at the surface. For InAs, ϕ_s is roughly

TABLE I. Parameters used in the calculation described in the text. The last two values, from Ref. 7, are for bulk InAs since values for InMnAs are not available.

Parameter	Value	Ref.
N_s (4.2 K)	$1.0 \times 10^{16} \text{ cm}^{-3}$	4
N_s (290 K)	$2.1 \times 10^{17} \text{ cm}^{-3}$	4
μ_n (4.2 K)	$1300 \text{ cm}^2/\text{V s}$	4
μ_n (290 K)	$400 \text{ cm}^2/\text{V s}$	4
E_G	0.334 eV	21
ϕ	0.167 V	23
L	150 nm	7
ϵ	12.25	7

equal to half of the band gap.²³ By approximating $N_n/\nabla N_n = N_p/\nabla N_p = L \approx 150 \text{ nm}$, the optical absorption length,⁹ we have the ratio of the magnitudes of the drift and diffusion currents as

$$\frac{J_D}{J_E} = \frac{k_B}{eLE_s} \left[\frac{T_n N_n \mu_n - T_p N_p \mu_p}{N_n \mu_n + N_p \mu_p} \right] \approx \frac{k_B T_n}{eLE_s}, \quad (4)$$

where we have used the approximation $\mu_p \approx 0$. Applying this model to our *n*-InMnAs sample (see Table I), we find that $J_D/J_E \approx 0.54$ at 300 K and $J_D/J_E \approx 2.45$ at 4 K. In other words, this simple model predicts a crossover point where $J_D = J_E$ at an intermediate lattice temperature T_X . In this approximate expression for J_D/J_E , only the static carrier density N_s [Eq. (3)] depends on the lattice temperature, with the high- and low-temperature limiting values given in Table I for our sample. By assuming that this static carrier density varies linearly with temperature, we can extrapolate a lattice temperature at which $J_D = J_E$, where we would expect the emitted terahertz field to vanish. The extrapolated value, $T_X \sim 75 \text{ K}$, is reasonably consistent with the experimentally determined crossover temperature of $\sim 70 \text{ K}$ (see Fig. 3).

The fact that our InMnAs samples are fabricated by low-temperature molecular beam epitaxy (MBE), while our reference *p*-InAs sample is not, could also be a contributing factor in the observed emission behavior. One could imagine that the observed polarity reversal is related to a temperature-dependent rate for carrier trapping at antisite defects introduced by low-temperature (LT) growth, which could influence the temperature dependence of the mobility. Future measurements on LT-InAs should provide information on the strength of the temperature dependence and its relation to the defects introduced by LT MBE growth.

In conclusion, we demonstrate terahertz emission from *p*-InMnAs and *n*-InMnAs. Both samples exhibit a polarity

reversal of the emitted terahertz field as a function of temperature. This phenomenon does not occur in *p*-InAs, which suggests that it is related to the influence of the Mn dopant on the carrier dynamics in these materials.

This work has been supported in part by the R. A. Welch Foundation, the American Chemical Society Petroleum Research Fund, the National Science Foundation, and the Intelligence Community Postdoctoral Fellowship Program. We also acknowledge the assistance of X.-C. Zhang, M. Fitch, and R. Osiander for supplying the *p*-InAs sample.

¹H. MuneKata, H. Ohno, S. von Molnar, A. Segmuller, L. L. Chang, and L. Esaki, Phys. Rev. Lett. **63**, 1849 (1989).

²H. Ohno, H. MuneKata, T. Penney, S. von Molnar, and L. L. Chang, Phys. Rev. Lett. **68**, 2664 (1992).

³J. Wang, C. Sun, J. Kono, A. Oiwa, H. MuneKata, L. Cywinski, and L. J. Sham, Phys. Rev. Lett. **95**, 167401 (2005).

⁴M. A. Zudov, J. Kono, Y. H. Matsuda, T. Ikaida, N. Miura, H. MuneKata, G. D. Sanders, Y. Sun, and C. J. Stanton, Phys. Rev. B **66**, 161307 (2002).

⁵S. Kono, P. Gu, M. Tani, and K. Sakai, Appl. Phys. B: Lasers Opt. **71**, 601 (2000).

⁶P. Gu, M. Tani, S. Kono, K. Sakai, and X.-C. Zhang, J. Appl. Phys. **91**, 5533 (2002).

⁷K. Liu, J. Xu, T. Yuan, and X.-C. Zhang, Phys. Rev. B **73**, 155330 (2006).

⁸M. Nakajima, M. Hangyo, M. Ohta, and H. Miyazaki, Phys. Rev. B **67**, 195308 (2003).

⁹J. N. Heyman, N. Coates, and A. Reinhardt, Appl. Phys. Lett. **83**, 5476 (2003).

¹⁰R. Ascazubi, I. Wilke, K. J. Kim, and P. Dutta, Phys. Rev. B **74**, 075323 (2006).

¹¹M. B. Johnston, D. M. Whittaker, A. Corchia, A. G. Davies, and E. H. Linfield, Phys. Rev. B **65**, 165301 (2002).

¹²N. Sarukara, H. Ohtake, S. Izumida, and Z. Liu, J. Appl. Phys. **84**, 654 (1998).

¹³R. McLaughlin, A. Corchia, M. B. Johnston, Q. Chen, C. M. Ciesla, D. D. Arnone, G. A. C. Jones, E. H. Linfield, A. G. Davies, and M. Pepper, Appl. Phys. Lett. **76**, 2038 (2000).

¹⁴C. Weiss, R. Wallenstein, and R. Beigang, Appl. Phys. Lett. **77**, 4160 (2000).

¹⁵J. Shan, C. Weiss, R. Wallenstein, R. Beigang, and T. F. Heinz, Opt. Lett. **26**, 849 (2001).

¹⁶J. N. Heyman, P. Neocleous, D. Hebert, P. A. Crowell, T. Muller, and K. Unterrainer, Phys. Rev. B **64**, 085202 (2001).

¹⁷D. J. Hilton, R. D. Averitt, C. A. Meserole, G. L. Fisher, D. J. Funk, J. D. Thompson, and A. J. Taylor, Opt. Lett. **29**, 1805 (2004).

¹⁸E. Beaureparie, G. M. Turner, S. M. Harrel, M. C. Beard, J.-Y. Bigot, and C. A. Schmuttenmaer, Appl. Phys. Lett. **84**, 3465 (2004).

¹⁹J. B. Heroux, Y. Ino, M. Kuwata-Gonokami, Y. Hashimoto, and S. Katsunoto, Appl. Phys. Lett. **88**, 221110 (2006).

²⁰M. Noguchi, K. Hirakawa, and T. Ikoma, Phys. Rev. Lett. **66**, 2243 (1991).

²¹L. O. Olsson, C. B. M. Andersson, M. C. Hakansson, J. Kanski, L. Ilver, and U. O. Karlsson, Phys. Rev. Lett. **76**, 3626 (1996).

²²B. B. Hu, A. S. Weling, D. H. Auston, A. V. Kuznetsov, and C. J. Stanton, Phys. Rev. B **49**, 2234 (1994).

²³W. Gudat and D. E. Eastman, J. Vac. Sci. Technol. **13**, 831 (1976).